The Astrophysical Journal, 654:93–98, 2007 January 1

STATISTICS OF QUASARS MULTIPLY IMAGED BY GALAXY CLUSTERS

Joseph F. Hennawi,[1,2,3] Neal Dalal,[1,4] and Paul Bode[3]
Received 2005 June 7; accepted 2006 August 31

ABSTRACT

We compute the expected number of quasars multiply imaged by cluster-size dark halos for current wide-field quasar surveys by carrying out a large ensemble of ray-tracing simulations through clusters from a cosmological N-body simulation of the ΛCDM cosmology, with power spectrum normalization $\sigma_8 = 0.95$. Our calculation predicts ∼4 quasar lenses with splittings $\theta > 10''$ in the SDSS spectroscopic quasar sample, consistent with the recent discovery of the wide separation lens SDSS J1004+4112, which has $\theta = 14.6''$. The SDSS faint photometric quasar survey will contain ∼12 multiply imaged quasars with splittings $\theta > 10''$. Of these, ∼2 will be lenses with $\theta > 30''$, and ∼2 will be at high redshift ($z_s \sim 4$).

Subject headings: galaxies: clusters: general — gravitational lensing — quasars: general

Online Material: color figures

1. INTRODUCTION

Strong gravitational lensing by clusters of galaxies provides a unique laboratory for studying the dark matter distribution in the largest collapsed structures in the universe. The most common manifestations of cluster strong lensing are giant arcs, which are highly elongated and sometimes multiply imaged background galaxies that have been distorted by the deep gravitational potential of a massive galaxy cluster. Background quasars can also be multiply imaged by foreground lenses. However, until recently, all of the roughly 70 lensed quasars known (Kochanek & Schechter 2004) had small $\theta \lesssim 10''$ separations, explained in terms of galaxy-scale concentrations of baryonic matter, despite a number of searches for lenses with wider splittings (Maoz et al. 1997; Ofek et al. 2001; Phillips et al. 2001; Zhdanov & Surdej 2001; Miller et al. 2004; Marble et al. 2004).

The discovery of the quadruply imaged quasar SDSS J1004+4112 (Inada et al. 2003, 2005; Oguri et al. 2004) in the Sloan Digital Sky Survey (SDSS), with a largest image separation of $\theta = 14.6''$, constitutes the first quasar multiply imaged by a cluster where dark matter dominates the lensing potential (Oguri et al. 2004). Quasars lensed by clusters are much rarer than giant arcs simply because the number density of quasars behind clusters is much lower than that of galaxies. Because massive clusters capable of strong lensing are also very rare, large samples of quasars are required to find quasars multiply imaged by clusters.

The advent of large-area digital imaging and spectroscopic surveys, like the SDSS (York et al. 2000) and the Two Degree Field Quasar Survey (Croom et al. 2004), has dramatically increased the number of known quasars. Although a spectroscopic survey of ∼30,000 quasars was required to discover one multiply imaged quasar lensed by a cluster (Inada et al. 2003; Oguri et al. 2004), new *photometric* quasar selection techniques applied to the current SDSS imaging data promise to yield as many as a million quasars (Richards et al. 2004). In addition, future large-area synoptic surveys such as the Panoramic Survey Telescope and Rapid Response System (Pan-STARRS) and the Large Synoptic Survey Telescope (LSST) will be able to use variability selection techniques to detect as many as one hundred million quasars. The number of quasars lensed by clusters discovered in these current and future samples of quasars will allow statistical studies of the abundance of these large separation quasar lenses.

It has been suggested that the abundance of cluster lenses can be used as a cosmological probe. Bartelmann et al. (1998) found that the predicted number of giant arcs varies by orders of magnitude among different cosmological models, and Bartelmann et al. (2003) and Meneghetti et al. (2005) recently proposed that giant arc statistics could be used to distinguish between different dark energy cosmological models. Despite the fact that the abundance of quasars lensed by clusters will be significantly lower, because quasars are point sources, the selection function of multiply imaged quasars is much easier to quantify than that of giant arcs, because the ability to detect giant arcs is extremely sensitive to the seeing. Indeed, beginning with Kochanek (1996) the abundance of multiply imaged quasars has been recognized as a potentially powerful cosmological probe. However, the dominant uncertainty has always been the accuracy with which the galaxy population can be modeled. Because on cluster scales only dark matter and gravity are involved, quasars multiply imaged by clusters would not suffer from these modeling uncertainties.

The measurement of a time delay in multiply imaged quasar cluster lenses could prove to be promising method for measuring the Hubble constant, if the cluster lens *also shows giant arcs*. This is because there would be more constraints on the mass model than are present in galaxy lenses, and it is precisely this modeling uncertainty that limits the precision of this technique (see e.g., Kochanek 2003; Kochanek & Schechter 2004). Finally, because multiply imaged quasar lenses are found by searching for pairs of quasars at the same redshift (that is, by surveying the source population), whereas giant arcs are discovered by looking for elongated structures in the vicinity of rich galaxy clusters (that is, by surveying the lens population), the two types of cluster lens surveys are complementary.

Nearly all previous investigations of the abundance of quasars lensed by massive dark halos have used simple spherically symmetric analytical profiles for the mass distribution of clusters to predict the abundance of wide separation quasar lenses (Maoz et al. 1997; Sarbu et al. 2001; Keeton & Madau 2001; Wyithe et al. 2001; Li & Ostriker 2002, 2003; Rusin 2002; Oguri 2003, 2004; Huterer & Ma 2004; Lopes & Miller 2004; Kuhlen et al. 2004; Chen 2004). However, in the context of giant arc statistics, full

[1] Hubble Fellow.
[2] Department of Astronomy, University of California, Berkeley, CA.
[3] Princeton University Observatory, Princeton, NJ.
[4] Institute for Advanced Study, Princeton, NJ.

ray-tracing computations through clusters from N-body simulations have unequivocally demonstrated that analytical models fail to accurately represent strong lensing by clusters (Bartelmann et al. 1995), underestimating the lensing cross sections by as much as 2 orders of magnitude (Meneghetti et al. 2003a; Hennawi et al. 2007). In recent progress, Oguri & Keeton (2004) computed the abundance of quasars multiply imaged by clusters analytically, using triaxial rather than spherical halos; they found that triaxiality significantly increases the expected number of lenses. In addition, all previous predictions for the number of wide separation multiply imaged quasar lenses have neglected the effect of the brightest cluster galaxies on the strong lensing cross section, focusing only on the effects of the dark matter. However, brightest cluster galaxies can enhance strong lensing cross sections by up to $\sim$50% (Meneghetti et al. 2003b; Dalal et al. 2004; Ho & White 2005; Hennawi et al. 2007) for small image separations ($\theta \lesssim 20''$).

In this paper we compute the expected number of quasars multiply imaged by cluster-size dark halos in current wide-field quasar surveys by carrying out a large ensemble of ray-tracing simulations through clusters from a large cosmological N-body simulation. In § 2, we briefly summarize the ray-tracing simulations and our technique for adding brightest cluster galaxies (BCGs) to dark matter halos. The details of the quasar luminosity functions for the surveys we consider are discussed in § 3. We present results on the abundance of quasars lensed by clusters in § 4, and we conclude in § 5.

2. RAY-TRACING SIMULATIONS

In this section, we briefly summarize the essential elements of our strong lensing simulations. We refer the reader to Dalal et al. (2004) and Hennawi et al. (2007) for details. We will discuss the N-body simulations, ray-tracing simulations, and our method for adding BCGs in turn.

In order to simulate the strong lensing effects of a universe filled with dark matter, we used clusters from a cosmological N-body simulation, performed with the tree particle-mesh (TPM) code of Bode & Ostriker (2003). The following cosmological parameters were used for this simulation: $\Omega_m = 0.3$, $\Omega_\Lambda = 0.7$, $h = 70$ km s^{-1} Mpc^{-1}, $\sigma_8 = 0.95$, and $n_s = 1$, which are consistent (within 1 σ) of the *WMAP*-derived cosmological parameters (Spergel et al. 2003). The simulations were performed in a box with a comoving side length of $L = 320\ h^{-1}$ Mpc and $N = 1024^3$ particles, giving a particle mass of $m_p = 2.54 \times 10^9\ h^{-1}\ M_\odot$. The cubic spline softening length was set to $\epsilon = 3.2\ h^{-1}$ kpc. We use outputs at seven different "snapshots," covering the range of redshifts over which the critical density is low enough to produce an appreciable amount of strong lensing: $z = 0.17, 0.29, 0.41, 0.55, 0.70, 0.87, 1.05, 1.26$, and 1.49. This same simulation has been used to investigate the statistics of giant arcs (Wambsganss et al. 2004; Hennawi et al. 2007), strong lensing cosmography (Dalal et al. 2005), and the lensing effects of secondary matter in the light cone (Wambsganss et al. 2005).

A "friends-of-friends" (FOF) group finder (Davis et al. 1985) with the canonical linking length of $b = 0.2$ was applied to each particle distribution to identify cluster-size dark matter halos. For each cluster with a FOF group mass above $M_{\rm FOF} \geq 10^{14}\ h^{-1}\ M_\odot$, all the particles within a 5 h^{-1} Mpc sphere about the center of mass were dumped to separate files and used as inputs to our ray-tracing code.

To compute reliable mean cross sections for a cluster, we must average over many projections to appropriately sample the distribution of cross sections (Dalal et al. 2004; Ho & White 2005; Hennawi et al. 2007). We computed mean lensing cross sections by averaging over 125 orientations for all clusters with $M_{\rm FOF} \geq 10^{15.0}\ h^{-1}\ M_\odot$, 31 orientations for clusters in the mass interval $10^{14.5}\ h^{-1}\ M_\odot \leq M_{\rm FOF} < 10^{15.0}\ h^{-1}\ M_\odot$, and 3 orientations for all clusters in the range $10^{14}\ h^{-1}\ M_\odot \leq M_{\rm FOF} < 10^{14.5}\ h^{-1}\ M_\odot$.

The surface density of each cluster projection is computed on a grid and a deflection angle map is computed using fast Fourier transform (FFT) methods. Using linked lists, a mapping is constructed between source plane pixels and image plane pixels. We then compute the statistics of multiply imaged quasars using a Monte Carlo approach. Single-pixel sources are randomly placed in the source plane. If there is more than one image plane pixel corresponding to this source plane pixel we count this as a multiply imaged quasar. If the image multiplicity is larger than 2, the separation of the images is taken to be the largest image separation in the system, and this is considered a single lensing event; thus we properly count triples, quads, etc. The magnifications of each image are also computed, which is just the ratio of the number of pixels in each image to the original number in the source (which is unity).

Given this list of image splittings and magnifications, the number of multiply imaged quasars behind each cluster orientation can be computed, given the number counts of background quasars as a function of apparent magnitude. Our calculation completely accounts for the magnification bias because we use the magnification of each image to determine the corresponding number density of background sources for the particular survey under consideration.

The ray-trace and Monte Carlo simulations must be repeated for each projection through the cluster and each source plane considered. We ray-trace three source planes at $z_s = 1.0, 2.0$, and 4.0. The number counts of quasars are thus collapsed into three source redshift bins centered on these source planes (see § 3), given by $[0.75, 1.5]$, $[1.5, 3.0]$, and $[3.0, 5.0]$, respectively. Because the critical density for strong lensing is a slowly varying function of source redshift, this binning will not introduce significant errors in our calculation.

BCGs can enhance strong lensing cross sections by $\sim$50% (Meneghetti et al. 2003b; Dalal et al. 2004; Ho & White 2005; Hennawi et al. 2007) for multiply imaged quasar separations $\lesssim 20''$, small enough such that the mass enclosed by the critical lines has a significant baryonic component (Dalal et al. 2004; Ho & White 2005; Hennawi et al. 2007). Indeed, the recently discovered wide separation quadruply imaged quasar lens SDSS J1004+4112 (Inada et al. 2003) is centered on the brightest galaxy of the cluster. Models of the lens that include the central galaxy embedded in a dark matter halo give an Einstein radius of $\sim 7''$, with the galaxy component contributing a significant amount to the lensing potential (Oguri et al. 2004).

We artificially add baryons, with a singular isothermal sphere profile, to the centers of each cluster by "painting" BCGs onto the dark matter surface density. Because varying the total mass of the central galaxy has a negligible effect on the lensing cross section (Dalal et al. 2004), we use a fixed fraction, $M_{\rm baryon} = 0.003 M_{\rm FOF}$, of the mass of the dark halo. We use a simple scaling prescription for assigning velocity dispersions to the BCGs

$$\frac{\sigma}{300\ \mathrm{km\ s^{-1}}} = \left(\frac{M_{\rm FOF}}{10^{15}\ h^{-1}\ M_\odot}\right)^{2/15}, \tag{1}$$

which is based on an empirical scaling relation between the optical luminosity of BCGs and the X-ray temperatures of galaxy clusters (Edge & Stewart 1991) and the fact that BCGs lie on the

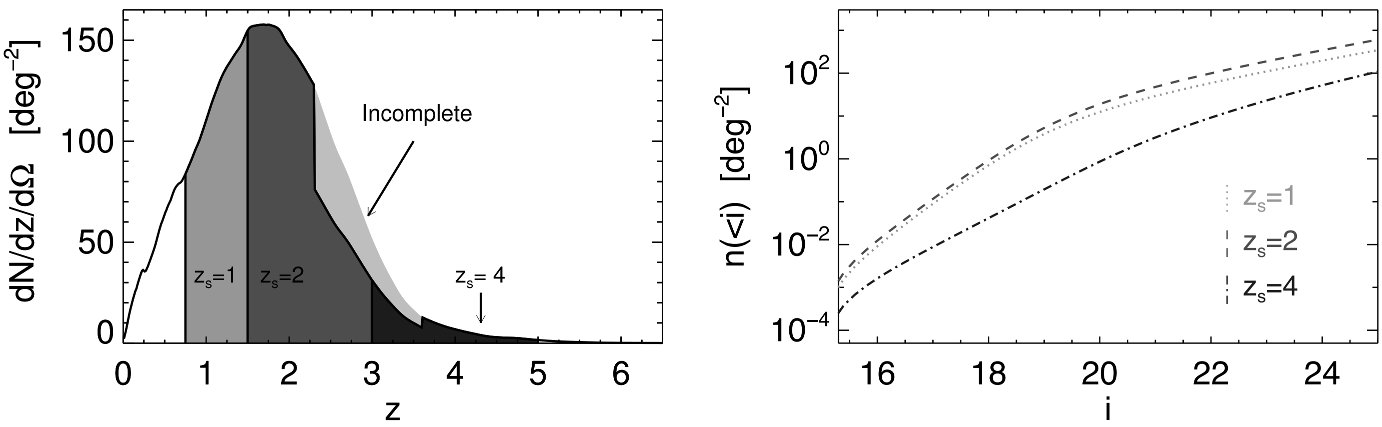

FIG. 1.—*Left*: Redshift distribution of quasars for a flux limit of $i < 22.7$. The shaded regions indicate the redshift bins used to determine the number of quasars for each of the three source planes at $z_s = 1$, 2, and 4. The area shaded light gray represents the number of quasars excluded by our assumption of 60% completeness over the redshift range $2.3 < z < 3.6$, where color-selected samples are incomplete because quasar colors cross the stellar locus. *Right*: Cumulative number magnitude counts of quasars used for each of our three source planes. These curves were obtained by integrating the redshift distribution of quasars over redshift bins illustrated by the shading in the left panel. [*See the electronic edition of the Journal for a color version of this figure.*]

fundamental plane of elliptical galaxies (Oegerle & Hoessel 1991). See Hennawi et al. (2007) for details.

3. MODELING THE QUASAR LUMINOSITY FUNCTION

We compute the expected abundance of wide separation multiply imaged quasars for two surveys: the SDSS spectroscopic survey (Schneider et al. 2005) and the fainter SDSS photometric quasar sample of Richards et al. (2004). At low redshift $z < 2.3$, the quasar luminosity function has been measured by several groups (Boyle et al. 2000; Croom et al. 2004; Richards et al. 2005). We use the double power-law B-band luminosity function (Boyle et al. 2000)

$$\Phi(M_B, z) = \frac{\Phi_*}{10^{0.4(\beta_l+1)[M_B-M_B^*(z)]} + 10^{0.4(\beta_h+1)[M_B-M_B^*(z)]}}, \qquad (2)$$

where $\beta_l = -1.64$, $\beta_h = -3.43$, and $\Phi_* = 360(h/0.50)^3$ Gpc^{-3} mag^{-1}. The evolution of the break luminosity $M_B^*(z)$ follows

$$M_B^* = M_B^*(0) - 2.5\left(k_1 z + k_2 z^2\right), \qquad (3)$$

with $k_1 = 1.36$, $k_2 = -0.27$, and $M_B^*(0) = -21.15 + 5\log h$.

The quasar luminosity function is poorly constrained between redshifts $2.3 \leq z \leq 3.6$. Wyithe & Loeb (2002) used a simple analytical model to fit the double power-law luminosity function in equation (2) to both the Fan et al. (2001) high-redshift ($z > 3.6$) luminosity function and the Boyle et al. (2000) low redshift ($z < 2.3$) luminosity function, using a model for the evolution of the break luminosity proposed by Madau et al. (1999),

$$L_B^*(z) = L_B^*(0)(1+z)^{(\alpha-1)} \frac{e^{\zeta z}(1+e^{\xi z_*})}{e^{\xi z} + e^{\xi z_*}}, \qquad (4)$$

where $\alpha = -0.5$ is the slope of a power-law spectral energy distribution assumed for the quasar spectrum $f_\nu \sim \nu^\alpha$. At the bright end they used the Fan et al. (2001) slope $\beta_h = 2.58$ and assumed a faint-end slope $\beta_l = 1.64$. The other parameters of their fit are $\Phi_* = 624$ Gpc^{-3} mag^{-1}, $M_B^*(0) = -22.46$, $z_* = 1.60$, $\zeta = 2.65$, and $\xi = 3.30$. This prescription for the luminosity function has also been employed in strong lensing studies by Oguri et al. (2004) and Oguri & Keeton (2004). For redshifts $z < 2.3$ we use the Boyle et al. (2000) expression in equation (2). In the range $2.3 < z < 3.6$ we linearly interpolate between equation (2) and the (Wyithe & Loeb 2002) fit, and we use the (Wyithe & Loeb 2002) fit for $z > 3.6$.

The luminosity functions we are considering are expressed in terms of rest frame B-band absolute magnitude, M_B, whereas the SDSS spectroscopic and photometric surveys have flux limits in the i-band. We thus require the cross filter K-correction $K_{Bi}(z)$, between apparent magnitude i and absolute magnitude B (see e.g., Hogg et al. 2002) to be

$$M_B^i = i - \mathrm{DM}(z) - K_{Bi}(z), \qquad (5)$$

where DM(z) is the distance modulus. We compute $K_{Bi}(z)$ from the SDSS composite quasar spectrum of Vanden Berk et al. (2001) and the Johnson B and SDSS i filter curves.

Between redshifts $2.3 \leq z \leq 3.6$, quasar surveys that rely on color selection suffer from incompleteness because quasar colors cross the stellar locus (see e.g., Richards et al. 2001; Vanden Berk et al. 2005) in this redshift range. Because the SDSS spectroscopic and photometric surveys rely on color selection, we conservatively assume that only 60% of the quasars in this interval are recovered, accounting for this incompleteness.

An area of $\sim$5000 deg^2 is assumed for the SDSS spectroscopic quasar survey, which has flux limits $i < 19.1$ for low redshift quasars ($z < 2.5$) and $i < 20.2$ for high-redshift quasars ($z > 2.5$; Schneider et al. 2005). We assume the faint photometric quasar survey covers the larger SDSS imaging area of $\sim$8000 deg^2, with flux limits $i < 21.0$ for $z < 2.5$ and $i < 20.5$ for $z > 2.5$ (Richards et al. 2004). The resulting total number of quasars are $\sim$69,000 and 629,000 for the spectroscopic survey and photometric survey, respectively.

Searching for quasar lenses requires follow-up observations. This is the case for the SDSS spectroscopic sample because of "fiber collisions,"[5] and also for the faint photometric sample because spectroscopy is required to confirm that two quasars in a pair are quasars at the same redshift, rather than a projected pair of quasars or stellar contaminants. The flux limit of the follow-up

[5] The finite size of the optical fibers of the SDSS multi-object spectrograph implies that only one quasar in a close pair with separation <55″ can have a spectrum in the quasar catalog.

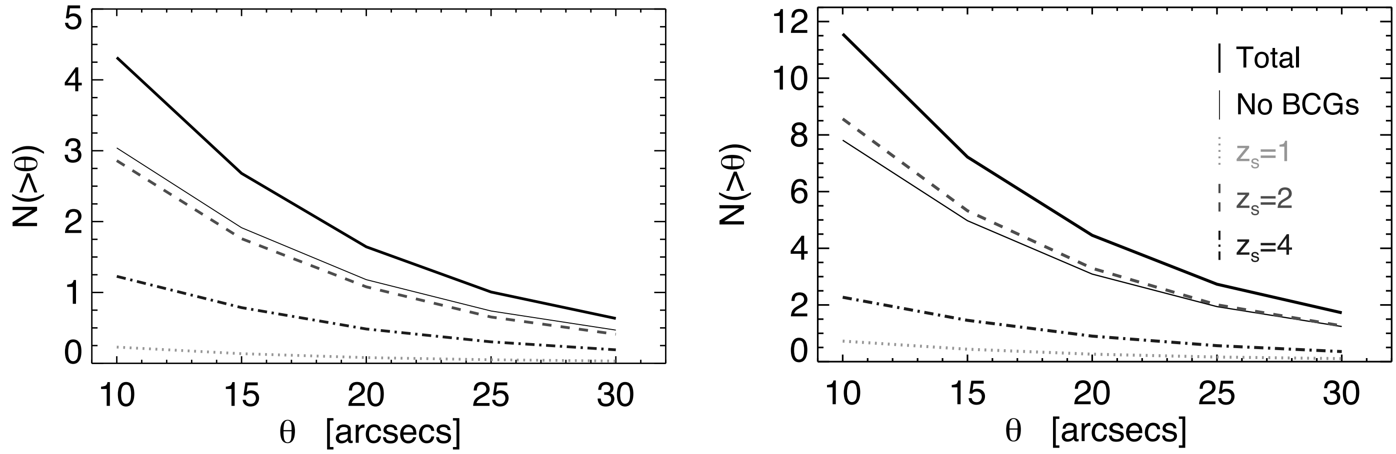

FIG. 2.—Cumulative distribution of image splittings for two different quasar surveys. The left panel is for the SDSS spectroscopic quasars and the right panel is for SDSS photometric quasar sample of Richards et al. (2004). The dotted, dashed, and dot-dashed curves are the separate contributions from the source planes at $z_s = 1.0$, 2.0, and 4.0, respectively. The sum of these three curves gives the total number of multiply imaged quasars (*heavy solid curve*). The light solid line shows the total number of lenses if BCGs are neglected and we ray-trace through dark matter only. [*See the electronic edition of the Journal for a color version of this figure.*]

observations is set by the follow-up instrument and is typically fainter than the flux limit of the parent sample. Thus for both surveys, we assume a flux limit of $i < 21$ for the fainter quasar in the pair, appropriate for follow up spectroscopy with a 4 m class telescope.

The left panel of Figure 1 shows the redshift distribution of quasars for a flux limit of $i < 22.7$, i.e., 2.5 mag fainter than the SDSS flux limit[6] of $i < 20.2$, corresponding to magnifications $\sim$10. The redshift bins used for each source plane are indicated by the shading. The right panel of Figure 1 shows the cumulative number magnitude counts of quasars in the redshift bins about each of the three source planes.

4. THE NUMBER OF QUASARS LENSED BY CLUSTERS

The expected cumulative distribution of lens splittings $N(>\theta)$ for the SDSS spectroscopic quasar survey and the SDSS photometric survey are shown in Figure 2. The dotted, dashed, and dot-dashed lines show the individual contributions from the source planes $z_s = 1.0$, $z_s = 2.0$, and $z_s = 4.0$, respectively. The heavy solid lines shows the total number of lenses, which is just the sum from the three individual source planes. The light solid line shows the total number of lenses if the baryons in BCGs are neglected and we ray-trace through dark matter only.

BCGs increase the number of lenses by $\sim$50%, consistent with previous findings (Meneghetti et al. 2003b; Dalal et al. 2004; Ho & White 2005; Hennawi et al. 2007). For the SDSS spectroscopic quasars, our results are consistent with the existence of one wide separation lensed quasar in the sample with a splitting $\theta \sim 14''$, namely SDSS J1004+4112. This lens was discovered in an effective area of $\sim$2500 deg^2 (Inada et al. 2003; Oguri et al. 2004), which is roughly half of that used in the left panel of Figure 2, so we would predict 1–2 such lenses in a quasar sample of this size. Our prediction of $\sim$4 quasar lenses with splittings $\theta > 10''$, suggests that several wide separation quasar lenses may still be lurking in the SDSS spectroscopic survey. For the faint photometric quasars, our calculation predicts $\sim$12 multiply imaged quasars with splittings $\theta > 10''$. It is expected that $\sim$2 lenses will have a separation $\theta > 30''$, and $\sim$2 wide separation lenses will be at $z_s \sim 4$.

At first glance, it seems unexpected that the number of quasar lenses in the photometric sample is only a factor of $\sim$3 higher than the spectroscopic sample, considering that the total number

[6] For the sake of illustration we have used a single flux limit in Fig. 1, although both quasar samples have different flux limits for high and low redshift.

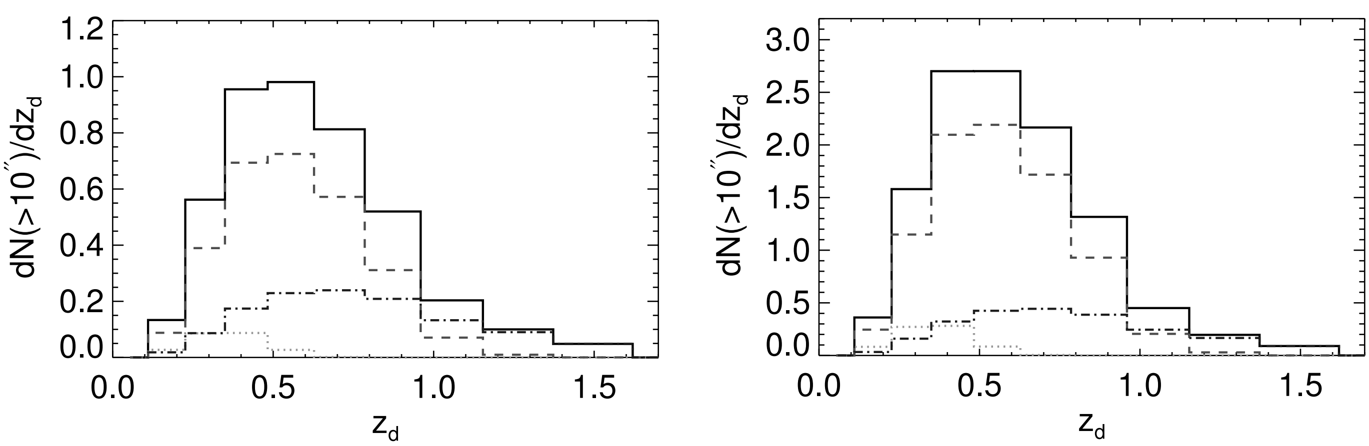

FIG. 3.—Redshift histogram of cluster lenses with splittings $\theta > 10''$ for the spectroscopic quasars (*left*) and photometric quasars (*right*). The dotted, dashed, and dot-dashed curves are the separate contributions from the source planes at $z_s = 1.0$, 2.0, and 4.0, respectively. The sum of these three curves gives the total number of multiply imaged quasars (*solid curve*). [*See the electronic edition of the Journal for a color version of this figure.*]

of quasars increased by a factor of ∼9, owing to the higher surface density and larger area (Richards et al. 2004). First, recall that the flux limit of the faintest image in the lens, which is identified from follow-up observations, is the same for both samples, namely $i < 21$. Most of the lensing probability is in the source bins $z_s = 2.0$ and $z_s = 4.0$, and the SDSS spectroscopic survey flux limit for these bins is already $i < 20.2$, compared to $i < 21.0$ for $z_s = 2.0$ and $i < 20.5$ for $z_s = 4.0$ in the photometric sample. Second, because the slope of the luminosity function becomes shallower at fainter magnitudes, magnification bias is not as important for the fainter photometric sample than it is for the spectroscopic sample. Thus the fainter flux limits of the photometric sample do not increase the number of lenses as much as naively expected.

In Figure 3 we show the redshift distribution of the cluster lenses with $\theta > 10''$ for both surveys. The lens redshift distribution peaks around $z_d = 0.5$. Although the efficiency for strong lensing peaks at half distance to the source plane, which is at $z_d = 0.75$ for the dominant source plane $z_s = 2.0$, the distribution is skewed toward the observer by the cluster mass function. Our results for the redshift distribution of the SDSS cluster lenses is consistent with the redshift, $z_s = 0.68$, of the cluster multiply imaging SDSS J1004+4112.

5. SUMMARY AND CONCLUSIONS

We consider the following to be the primary conclusions of this study:

1. Our ray-tracing calculation through clusters from an *N*-body simulation of the ΛCDM cosmology predicts ∼4 quasar lenses with splittings $\theta > 10''$ in the SDSS spectroscopic quasar sample, consistent with the recent discovery of the wide separation lens SDSS J1004+4112, which has $\theta = 14.6''$.
2. Our study predicts ∼12 multiply imaged quasars with splittings $\theta > 10''$ should be found in the faint photometric quasar sample of Richards et al. (2004). Of these, ∼2 should be lenses with $\theta > 30''$ and ∼2 will be at high redshift $z_s \sim 4$.
3. BCGs increase the number of multiply imaged quasar lenses by ∼50%, consistent with previous findings in the context of giant arcs (Meneghetti et al. 2003b; Dalal et al. 2004; Ho & White 2005; Hennawi et al. 2007).

Before we conclude, it is worth discussing the dependence of the number of lensed quasars on the cosmological parameters. As has been noted previously (Oguri et al. 2004; Oguri & Keeton 2004), the dominant sensitivity is to the normalization of power spectrum fluctuations, σ_8, which arises because of the exponential sensitivity of the number density of massive clusters to this quantity. Our study considered $\sigma_8 = 0.95$, which is high compared to the *WMAP*-only best-fit $\sigma_8 = 0.84$ (Spergel et al. 2003), although consistent with it at the 1 σ level. To estimate how much our prediction depends on σ_8, we can determine the difference in the number density of massive clusters at the mass scale characteristic of multiply imaged quasar lenses. According to our simulations, 50% of the lensed quasars with image separations $>10''$ have a FOF mass of $M_{\rm FOF} \geq 3.7 \times 10^{14}\ h^{-1}\ M_\odot$. Using the mass function of Jenkins et al. (2001), we find that the cosmological model simulated here predicts 2.6 times more clusters per unit volume above this mass, $n(>3.7 \times 10^{14}\ h^{-1}\ M_\odot)$, than the *WMAP* model. The number of clusters would be 6.8 times higher than a model with *WMAP* parameters but a lower value of $\sigma_8 = 0.75$.

Oguri & Keeton (2004) argued that the existence of one multiply imaged quasar in the range $7'' \lesssim \theta \lesssim 60''$ (i.e., SDSS J1004+4112) in a sample of ∼29,000 SDSS spectroscopic quasars is consistent with CDM provided $\sigma_8 \sim 1$. Here we predicted ∼4 systems with $\theta \geq 10''$ in 70,000 spectroscopic quasars, which is larger than the Oguri & Keeton (2004) prediction by a factor of ∼2; however, Oguri & Keeton restricted their study to only quasars with $z < 2.2$. Furthermore, Hennawi et al. (2007) found that triaxial CDM halos underpredict the number of giant arcs by a factor of ∼30% compared to simulated clusters, and Oguri & Keeton studied triaxial models. These two factors probably explain why we predict a larger number of lenses.

The search for wide separation multiply imaged quasar lenses is currently underway in both the SDSS spectroscopic (Inada et al. 2003; Oguri et al. 2004, 2005; Hennawi et al. 2006) and photometric samples (Richards et al. 2004; Hennawi et al. 2006). Looking forward, wide-field synoptic surveys like Pan-STARRS and the LSST will be able to combine variability and color selection techniques to detect as many as 10^8 quasars down to $i \lesssim 27$ (R. Green 2004, private communication). Crudely extrapolating from the lensing rate computed here, these future surveys are likely to contain $\gtrsim$300 quasars multiply imaged by clusters. A comparison of the abundance of these new lenses to theoretical predictions as well as detailed modeling of each system, will provide a powerful test of the ΛCDM cosmological model.

We are grateful to Jerry Ostriker for reading an early version of this manuscript and providing helpful comments. We also wish to thank Jim Gunn, Richard Green, Donald Schneider, and Gordon Richards for helpful discussions. J. F. H. would like to thank his thesis advisors David Spergel and Michael Strauss for advice and guidance during his time in Princeton, where this work was started. For part of this study J. F. H. was supported by Proctor Graduate fellowship at Princeton University and by a generous gift from the Paul and Daisy Soros Fellowship for New Americans. The program is not responsible for the views expressed. J. F. H. and N. D. are supported by NASA through Hubble Fellowship grants 01172.01-A and 01148.01-A, respectively, awarded by the Space Telescope Science Institute, which is operated by the Association of Universities for Research in Astronomy, Inc., for NASA, under contract NAS 5-26555. Computer time was provided by the National Computational Science Alliance under program MCA04N002P, and some computations were performed on the NSF Terascale Computing System at the Pittsburgh Supercomputing Center. The ray-tracing simulations used computational facilities at Princeton supported by NSF grant AST-0216105.

REFERENCES

Bartelmann, M., Huss, A., Colberg, J. M., Jenkins, A., & Pearce, F. R. 1998, A&A, 330, 1
Bartelmann, M., Meneghetti, M., Perrotta, F., Baccigalupi, C., & Moscardini, L. 2003, A&A, 409, 449
Bartelmann, M., Steinmetz, M., & Weiss, A. 1995, A&A, 297, 1
Bode, P., & Ostriker, J. P. 2003, ApJS, 145, 1
Boyle, B. J., Shanks, T., Croom, S. M., Smith, R. J., Miller, L., Loaring, N., & Heymans, C. 2000, MNRAS, 317, 1014
Chen, D.-M. 2004, A&A, 418, 387
Croom, S. M., Smith, R. J., Boyle, B. J., Shanks, T., Miller, L., Outram, P. J., & Loaring, N. S. 2004, MNRAS, 349, 1397
Dalal, N., Hennawi, J. F., & Bode, P. 2005, ApJ, 622, 99
Dalal, N., Holder, G., & Hennawi, J. F. 2004, ApJ, 609, 50
Davis, M., Efstathiou, G., Frenk, C. S., & White, S. D. M. 1985, ApJ, 292, 371
Edge, A. C., & Stewart, G. C. 1991, MNRAS, 252, 428
Fan, X., et al. 2001, AJ, 121, 54
Hennawi, J. F., Dalal, N., Bode, P., & Ostriker, J. P. 2007, ApJ, 654, 714
Hennawi, J. F., et al. 2006, AJ, 131, 1

Ho, S., & White, M. 2005, Astropart. Phys., 24, 257
Hogg, D. W., Baldry, I. K., Blanton, M. R., & Eisenstein, D. J. 2002, preprint (astro-ph/0210394)
Huterer, D., & Ma, C. 2004, ApJ, 600, L7
Inada, N., et al. 2003, Nature, 426, 810
———. 2005, PASJ, 57, L7
Jenkins, A., Frenk, C. S., White, S. D. M., Colberg, J. M., Cole, S., Evrard, A. E., Couchman, H. M. P., & Yoshida, N. 2001, MNRAS, 321, 372
Keeton, C. R., & Madau, P. 2001, ApJ, 549, L25
Kochanek, C. S. 1996, ApJ, 466, 638
———. 2003, ApJ, 583, 49
Kochanek, C. S., & Schechter, P. L. 2004, in Measuring and Modeling the Universe, ed. W. L. Freedman (Cambridge: Cambridge Univ. Press), 117
Kuhlen, M., Keeton, C. R., & Madau, P. 2004, ApJ, 601, 104
Li, L., & Ostriker, J. P. 2002, ApJ, 566, 652
———. 2003, ApJ, 595, 603
Lopes, A. M., & Miller, L. 2004, MNRAS, 348, 519
Madau, P., Haardt, F., & Rees, M. J. 1999, ApJ, 514, 648
Maoz, D., Rix, H., Gal-Yam, A., & Gould, A. 1997, ApJ, 486, 75
Marble, A. R., Impey, C. D., Miller, L., Clewley, L., Edmondson, E., & Lopes, A. M. 2004, BAAS, 205, 148.11
Meneghetti, M., Bartelmann, M., Dolag, K., Moscardini, L., Perrotta, F., Baccigalupi, C., & Tormen, G. 2005, NewA Rev., 49, 111
Meneghetti, M., Bartelmann, M., & Moscardini, L. 2003a, MNRAS, 340, 105
Meneghetti, M., Bartelmann, M., & Moscardini, L. 2003b, MNRAS, 346, 67
Miller, L., Lopes, A. M., Smith, R. J., Croom, S. M., Boyle, B. J., Shanks, T., & Outram, P. 2004, MNRAS, 348, 395
Oegerle, W. R., & Hoessel, J. G. 1991, ApJ, 375, 15
Ofek, E. O., Maoz, D., Prada, F., Kolatt, T., & Rix, H. 2001, MNRAS, 324, 463
Oguri, M. 2003, MNRAS, 339, L23
Oguri, M., & Keeton, C. R. 2004, ApJ, 610, 663
Oguri, M., et al. 2004, ApJ, 605, 78
———. 2005, ApJ, 622, 106
Phillips, P. M., et al. 2001, MNRAS, 328, 1001
Richards, G. T., et al. 2001, AJ, 121, 2308
———. 2004, ApJS, 155, 257
———. 2005, MNRAS, 360, 839
Rusin, D. 2002, ApJ, 572, 705
Sarbu, N., Rusin, D., & Ma, C. 2001, ApJ, 561, L147
Schneider, D. P., et al. 2005, AJ, 130, 367
Spergel, D. N., et al. 2003, ApJS, 148, 175
Vanden Berk, D. E., et al. 2001, AJ, 122, 549
———. 2005, AJ, 129, 2047
Wambsganss, J., Bode, P., & Ostriker, J. P. 2004, ApJ, 606, L93
———. 2005, ApJ, 635, L1
Wyithe, J. S. B., & Loeb, A. 2002, ApJ, 577, 57
Wyithe, J. S. B., Turner, E. L., & Spergel, D. N. 2001, ApJ, 555, 504
York, D. G., et al. 2000, AJ, 120, 1579
Zhdanov, V. I., & Surdej, J. 2001, A&A, 372, 1